ECS Transactions, 80 (7) 191-196 (2017)
10.1149/08007.0191ecst ©The Electrochemical Society

Growth and Characterization of α-, β-, and ε-Ga_2O_3 Epitaxial Layers on Sapphire

Y. Yao[a], L.A.M. Lyle[a], J.A. Rokholt[a], S. Okur[b], G.S. Tompa[b], T. Salagaj[b], N. Sbrockey[b], R.F. Davis[a], and L.M. Porter[a]

[a] Department of Materials Science & Engineering, Carnegie Mellon University, Pittsburgh, Pennsylvania 15213, USA
[b] Structured Materials Industries, Inc., Piscataway, New Jersey 08854, USA

This study reports on the growth and characterization of three different phases – α, β, and ε – of Ga_2O_3 epitaxial layers grown on (001) sapphire substrates at 650 °C. The stable β-phase was observed for films grown using metalorganic chemical vapor deposition with trimethygallium and oxygen as source gases. In contrast, the α- and/or ε-phase(s) were observed for films grown by halide vapor phase epitaxy with gallium chloride and oxygen as source gases. Orientation relationships from x-ray diffraction measurements are reported, along with transmission electron microscopy images of the interfacial microstructure and optical transmittance measurements of the different phases.

Introduction

To satisfy the surge in energy demand, there is an increasing need for high efficiency power electronics for energy conversion, such as for electrical switching within the electrical grid and for power supplies in electric vehicles. Although silicon devices have been traditionally used for power electronics, wide bandgap semiconductors are more efficient for these applications, because they can withstand higher electric fields with less material and energy loss. As an example, Toyota recently began trials of a new hybrid system using power electronics based on SiC and claims that power electronic devices based on SiC could increase fuel efficiency of hybrid vehicles by 10% (1). At present, 4H-SiC is the material of choice for both substrates and films for devices operating at and above 1200 volts. The upper limits of operation for power devices fabricated in GaN-based films are markedly lower. The substrates of both materials are produced by energy-intensive vapor-phase techniques and are still very expensive. A very promising alternative to SiC and GaN is gallium oxide, Ga_2O_3, which has an even larger bandgap. The recent availability of Ga_2O_3 single-crystal substrates produced from the melt presents new possibilities for devices that could translate to even greater energy efficiencies at lower cost than predicted for SiC and GaN. Furthermore, n-type doping (2), ohmic and Schottky contacts (3, 4), and various devices, such as MESFETs (5), MOSFETs (6), and UV solar-blind detectors (7) have already been demonstrated on Ga_2O_3.

Ga_2O_3 has been observed to exist in five polymorphs: α-, β-, γ-, δ-, and ε-phases (8). The monoclinic β-phase is the thermodynamically stable phase. Single crystals of the β-phase can be grown using inexpensive melt-growth methods, including edge-defined film fed (9), Czochralski (10, 11), Bridgman (12), and float-zone (2, 13). Polished 2-in

diameter wafers and oriented homoepitaxial films of β-Ga_2O_3 have recently become commercially available (14). However, there is increasing interest in the other phases, particularly the metastable corundum-structured α- and hexagonal-structured ε-Ga_2O_3 phases. The α- and ε-phases are of particular interest because of their higher symmetry and simpler epitaxial relations to c-plane sapphire. Both of these phases have been reported to grow as epitaxial films on oriented substrates (15-23).

In this paper we summarize our successful growth of epitaxial films of α-, β- and ε-phases on c-plane sapphire using different precursors and growth conditions. The α- and ε-phases have generally been reported in the literature to form at lower growth temperatures than the β-phase However, we observed a change in phase formation at the same growth temperature by changing our growth technique and Ga precursor from metalorganic chemical vapor deposition (MOCVD) and trimethlygallium to halide vapor phase epitaxy (HVPE) and gallium chloride. The HVPE method allowed a significantly higher growth rate than MOCVD and is, therefore, advantageous for growth of the very thick films needed in high-power devices. Data from x-ray diffraction (XRD), optical transmittance and cross-sectional transmission electron microscopy (TEM) are presented to illustrate the different epitaxial films.

Experimental Background

All of the epitaxial films in this study were grown in a vertical vapor phase epitaxy reactor at Structured Materials Industries, Inc. The reactor consists of a 16-inch diameter stainless steel chamber and a rotating disc reactor with a 13-inch platter. Gas flows from a showerhead at the top of the chamber. The epitaxial films were grown on single-side chemically-mechanically polished, 2-inch diameter, *c*-plane (001) sapphire (Al_2O_3) wafers that were obtained from a commercial vendor.

For the films grown by MOCVD, the chamber pressure and temperature were held at 45 Torr and 650 °C, respectively. These conditions were found in our previous studies to enhance growth rates (24, 25). Trimethylgallium (TMGa) at 85 sccm flow rate and O_2 at 2800 sccm were used as precursors; Ar at 10000 sccm was used as the carrier gas.

For the films grown by HVPE, the chamber pressure and temperature were maintained at 550 Torr and 650 °C, respectively. GaCl (produced by flowing 15% HCl in Ar at rates between 138 – 300 sccm over Ga metal held at a temperature of ~600 °C) was used as the Ga gas source precursor. O_2, at flow rates of 20 – 80 sccm, was used as the oxygen source. The growth time for all films was 30 min.

XRD θ-2θ scans were conducted using a Panalytical X'pert Pro MPD X-ray diffractometer with a Cu Kα X-ray source. Cross-sectional TEM images were obtained with a JEOL JEM-2000EX operating at 200kV and an FEI Titan G2 80-300 operating at 300kV. Optical transmittance measurements were conducted using an Optronic Laboratories OL 770 Multi-Channel Spectroradiometer with xenon light source and integrating sphere.

Results

Photos of (a) a 2-in diameter $(\bar{2}01)$ β-Ga_2O_3 wafer purchased from Tamura Corp. and (b) a 300-nm-thick, $(\bar{2}01)$ β-Ga_2O_3 epitaxial layer grown by MOCVD on a (001) sapphire wafer are shown in Fig. 1. Both wafers are transparent. The slight color tint in the Ga_2O_3 wafer (Fig. 1a) is attributed to the Sn (n-type) dopant impurities. In comparison, the undoped epitaxial layer grown on sapphire is transparent and colorless (Fig. 1b).

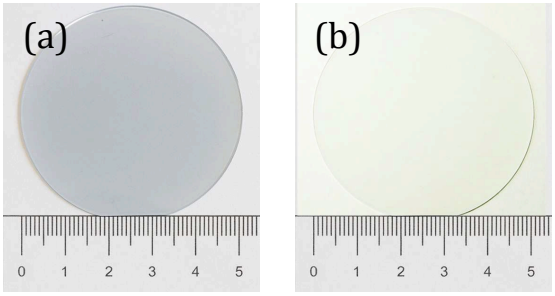

Figure 1. Photographs of (a) Sn-doped β-Ga_2O_3 wafer from Tamura Corp., Japan, and (b) undoped β-Ga_2O_3 epitaxial layer grown on a (001) sapphire wafer. (Numbers on rulers are in centimeters.)

A θ–2θ XRD spectrum (Fig. 2(a)) of an epitaxial film grown by MOCVD on (001) sapphire shows primary diffraction peaks from the set of $(\bar{2}01)$ planes. These results indicate that the film is $(\bar{2}01)$ oriented, which agrees with other reports for β-Ga_2O_3 grown on (001) sapphire substrates (23, 26, 27). When the film growth method was changed to HVPE, instead of β-Ga_2O_3, XRD characterization revealed the growth of (001)-oriented α-Ga_2O_3 (Fig. 2(b)) or (001)-oriented ε-Ga_2O_3 (Fig. 2(c)). We note that ε-Ga_2O_3 was detected in films grown with higher Ar flow rates and, correspondingly, faster film growth rates (~20 nm/min) – and typically thicker films – than those that resulted in α-Ga_2O_3. However, it should also be pointed out that the growth rates for all films grown by HVPE were at least 10x greater than growth rates for films grown by MOCVD and that HVPE source injection was not optimized. (We expect much higher growth rates to be possible with further optimization.)

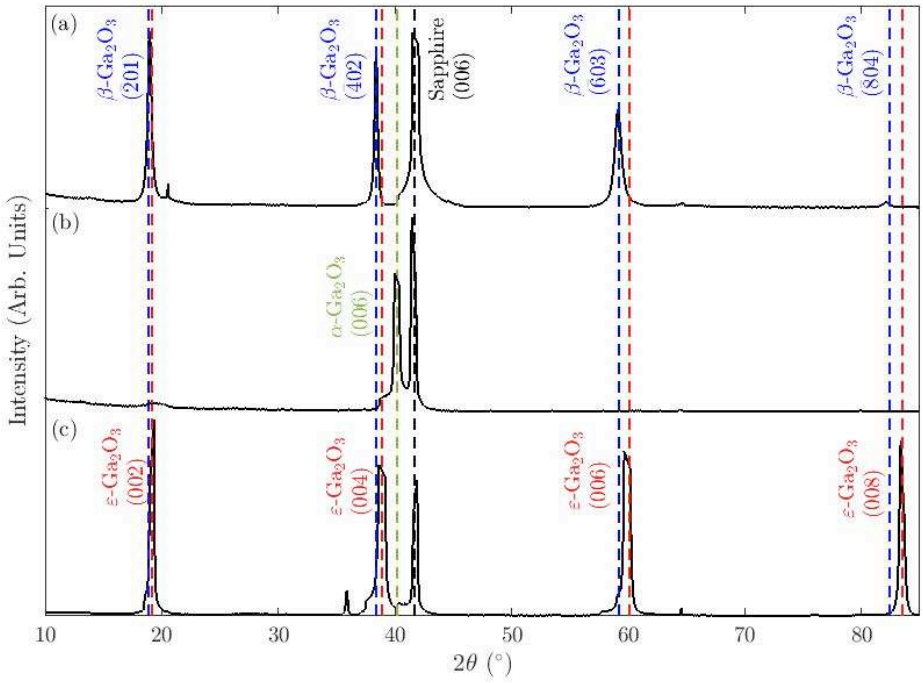

Figure 2. XRD θ-2θ scans of Ga_2O_3 epitaxial layers on (001) sapphire. (a) sample #47, grown by MOCVD; (b) sample #105, grown by HVPE; and (c) sample #108, grown by HVPE.

Cross-section TEM images show an abrupt interface between MOCVD grown β-Ga_2O_3 and sapphire (Fig. 3(a)). Whereas, cross-section TEM images of an HVPE grown film identified from XRD as ε-Ga_2O_3 showed that a 10–20 nm thick α-Ga_2O_3 epitaxial layer grew initially on the sapphire substrate, on top of which ε-Ga_2O_3 grew (Fig. 3(b)). The epitaxial relationship between the layers was determined from high resolution images and selected area diffraction patterns and are being reported elsewhere (28). The growth of these metastable phases may be associated with the faster growth rates, relatively low growth temperature, and/or impurity-induced film stress associated with the HVPE growth conditions employed. Additionally, it should be noted that the lattice mismatch between α-Ga_2O_3 and (001) sapphire is less than that between either β-Ga_2O_3 or ε-Ga_2O_3 and sapphire; therefore α-Ga_2O_3 appears to serve as a buffer layer in this case.

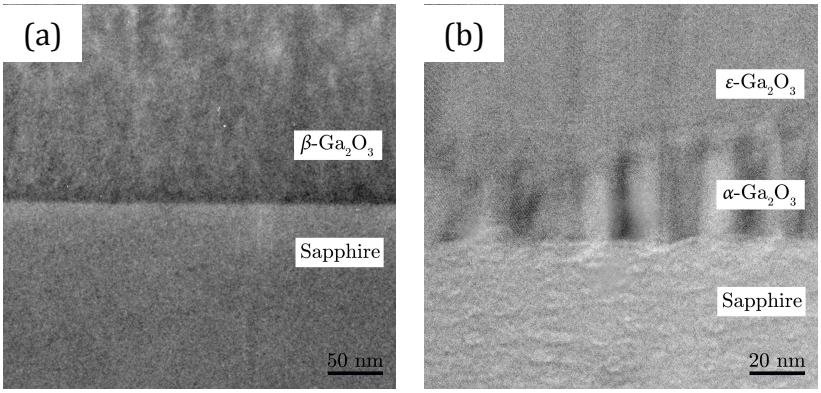

Figure 3. Cross-sectional TEM images of (a) β-Ga_2O_3 grown by MOCVD and (b) ε-Ga_2O_3/α-Ga_2O_3 grown by HVPE on (001) sapphire.

Optical transmittance measurements of α-, β-, and ε-Ga_2O_3 epitaxial films are compared in Fig. 4. Relatively sharp absorption cutoffs occur for all three phases. The cutoff for β-Ga_2O_3 occurs at ~250 nm, which corresponds within the range of reported bandgap values for β-Ga_2O_3 of 4.4–5.0 eV (29-32). This range in reported values has been attributed to optical anisotropy of β-Ga_2O_3 crystals (29). The absorption cutoff for the ε-Ga_2O_3 film was close to that of β-Ga_2O_3, whereas that for the α-Ga_2O_3 film was approximately 230-240 nm (5.2–5.4 eV).

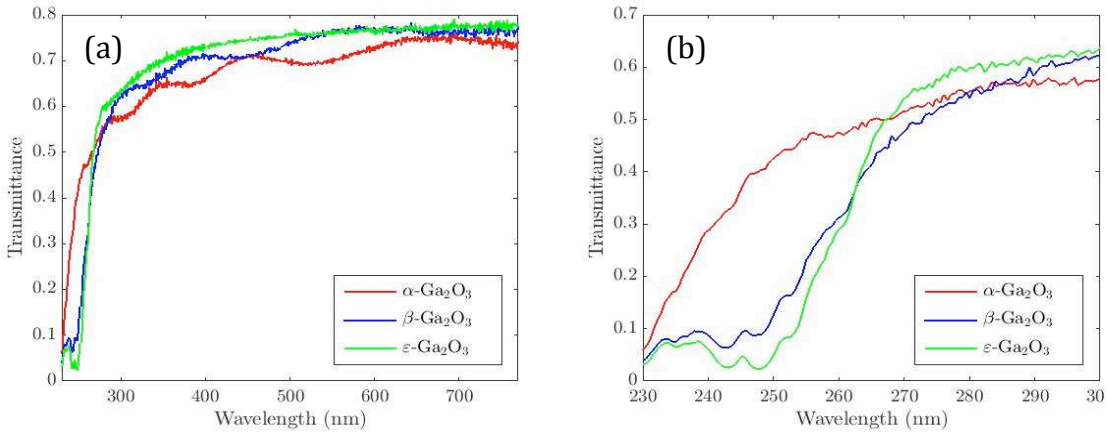

Figure 4. Transmittance curves of α-, β-, and ε-Ga_2O_3 epitaxial layers on (001) sapphire: (a) 250–800 nm; (b) zoomed in to show absorption edges in the UV.

Summary

This paper reported on growth conditions that yielded three different phases – α, β, and ε – of epitaxial Ga_2O_3 films on (001) sapphire substrates. XRD scans revealed the orientations of the films, and TEM showed microstructural details of the interfaces. Optical transmittance measurements showed a sharp absorption cutoff for all phases – with that for α-Ga_2O_3 appearing ~20 nm shorter in wavelength than that observed for the β- and ε-phases.

Acknowledgments

The authors acknowledge the Office of Naval Research under contract no. N00014-16-P2059 and the National Science Foundation under grant #ECCS-1642740 for support of this research. Use of the Materials Characterization Facility at Carnegie Mellon University was supported by grant MCF-677785.

References

1. S. Ashley *Efficient power electronics for hybrids and EVs*. Automotive Engineering, 2014.
2. N. Ueda, H. Hosono, R. Waseda and H. Kawazoe, *Appl. Phys. Lett.* **70**(26), 3561 (1997).
3. Y. Yao, R.F. Davis and L.M. Porter, *J. Electron. Mater.* **46**(4), 2053 (2016).
4. Y. Yao, R. Gangireddy, J. Kim, K. Das, R.F. Davis and L.M. Porter, *J. Vac. Sci. Technol. B*. **35**, 03D113.1 (2017).
5. M. Higashiwaki, K. Sasaki, A. Kuramata, T. Masui and S. Yamakoshi, *Appl. Phys. Lett.* **100**, 013504.1 (2012).
6. M. Higashiwaki, K. Sasaki, T. Kamimura, M.H. Wong, D. Krishnamurthy, A. Kuramata, T. Masui and S. Yamakoshi, *Appl. Phys. Lett.* **103**, 123511.1 (2013).
7. T. Oshima, T. Okuno, N. Arai, N. Suzuki, S. Ohira and S. Fujita, *Applied Physics Express*. **1**, 011202.1 (2008).
8. R. Roy, V.G. Hill and E.F. Osborn, *J. Am. Chem. Soc.* **74**(3), 719 (1952).
9. H. Aida, K. Nishiguchi, H. Takeda and N. Aota, *Jpn. J. Appl. Phys.* **47**(11), 8506 (2008).
10. Y. Tomm, P. Reiche, D. Klimm and T. Fukuda, *J. Crys. Growth*. **220**, 510 (2000).
11. Z. Galazka, R. Yecker, K. Irmscher, M. Albrecht, D. Klimm, M. Pietsch, M. Brützam, R. Bertram, S. Ganschow and R. Fornari, *Cryst. Res. Technol.* **45**(12), 1229 (2010).
12. K. Hoshikawa, E. Ohba, T. Kobayashi, J. Yanagisawa, C. Miyagawa and Y. Nakamura, *J. Cryst. Growth*. **447**, 36 (2016).
13. G. Villora, K. Shimamura, Y. Yoshikawa, K. Aoki and N. Ichinose, *J. Cryst. Growth*. **270**(3-4), 420 (2004).
14. Tamura Corporation, *Single-crystal gallium oxide substrates*, Tokyo, Japan: http://www.tamura-ss.co.jp/en/release/20131122/.
15. H. Nishinaka, D. Tahara and M. Yoshimoto, *Jpn. J. Appl. Phys.* **55**, 1202BC.1 (2016).
16. F. Mezzadri, G. Calestani, F. Boschi, D. Delmonte, M. Bosi and R. Fornari, *Inorg. Chem.* **55**(22), 12079 (2016).

17. F. Boschi, M. Bosi, T. Berzina, E. Buffagni, C. Ferrari and R. Fornari, *J. Cryst. Growth*. **443**, 25 (2016).
18. H. Akazawa, *Vacuum*. **123**, 8 (2016).
19. Y. Oshima, E.G. Villora and K. Shimamura, *Applied Physics Express*. **8**, 055501.1 (2015).
20. Y. Oshima, E.G. Villora, Y. Matsushita, S. Yamamoto and K. Shimamura, *J. Appl. Phys.* **118**, 085301.1 (2015).
21. R. Schewski, G. Wagner, M. Baldini, D. Gogova, Z. Galazka, T. Schulz, T. Remmele, T. Markurt, H. von Wenckstern and M. Grundmann, *Applied Physics Express*. **8**(1), 011101.1 (2014).
22. D. Shinohara and S. Fujita, *Jpn. J. Appl. Phys.* **47**(9), 7311 (2008).
23. T. Oshima, T. Okuno and S. Fujita, *Jpn. J. Appl. Phys.* **46**(11), 7217 (2007).
24. N.M. Sbrockey, T. Salagaj, E. Coleman, G.S. Tompa, Y. Moon and M.S. Kim, *J. Electron. Mater.* **44**(5), 1357 (2015).
25. S. Okur, G.S. Tompa, N.M. Sbrockey, T. Salagaj, V. Blank, B. Henninger, M. Baldini, G. Wagner, Z. Galazka, Y. Yao, J. Rokholt, R.F. Davis, L. Porter and A. Belkind, *Vacuum Technology & Coatings*. **May 2017**, 31 (2017).
26. S. Nakagomi and Y. Kokubun, *Phys. Stat. Sol. A*. **210**, 1738 (2013).
27. E.G. Villora, K. Shimamura and K. Kitamura, *Appl. Phys. Lett.* **88**, 031105.1 (2006).
28. Y. Yao, S. Okur, G.S. Tompa, T. Salagaj, N.M. Sbrockey, R.F. Davis and L.M. Porter, *To be submitted* (2017).
29. K.A. Mengle, G. Shi, D. Bayerl and E. Kioupakis, *Appl. Phys. Lett.* **109**, 212104.1 (2016).
30. H. He, R. Orlando, M.A. Blanco, R. Pandey, E. Amzallag, I. Baraille and M. Rérat, *Phys. Rev. B*. **74**(19), 195123.1 (2006).
31. M. Orita, H. Ohta, M. Hirano and H. Hosono, *Appl. Phys. Lett.* **77**(25), 4166 (2000).
32. H.H. Tippins, *Phys. Rev. A*. **140**, 316 (1965).